Structure and Stability Changes of Human IgG1 Fc as a Consequence of Methionine Oxidation

Dingjiang Liu,*,‡ Da Ren,‡ Holly Huang,‡ Jane Dankberg,‡ Robert Rosenfeld,§ Melanie J. Cocco,△ Luke Li,§ David N. Brems,‡ and Richard L. Remmele, Jr.‡

Department of Pharmaceutics, Amgen, Inc., Thousand Oaks, California 91320, Department of Protein Science, Amgen, Inc., Thousand Oaks, California 91320, and Department of Molecular Biology and Biochemistry, School of Biological Sciences, University of California, Irvine, California 92697-3900

Received November 9, 2007; Revised Manuscript Received February 7, 2008

ABSTRACT: The Fc region has two highly conserved methionine residues, Met 33 (C_H2 domain) and Met 209 (C_H3 domain), which are important for the Fc's structure and biological function. To understand the effect of methionine oxidation on the structure and stability of the human IgG1 Fc expressed in *Escherichia coli*, we have characterized the fully oxidized Fc using biophysical (DSC, CD, and NMR) and bioanalytical (SEC and RP-HPLC−MS) methods. Methionine oxidation resulted in a detectable secondary and tertiary structural alteration measured by circular dichroism. This is further supported by the NMR data. The HSQC spectral changes indicate the structures of both C_H2 and C_H3 domains are affected by methionine oxidation. The melting temperature (T_m) of the C_H2 domain of the human IgG1 Fc was significantly reduced upon methionine oxidation, while the melting temperature of the C_H3 domain was only affected slightly. The change in the C_H2 domain T_m depended on the extent of oxidation of both Met 33 and Met 209. This was confirmed by DSC analysis of methionine-oxidized samples of two site specific methionine mutants. When incubated at 45 °C, the oxidized Fc exhibited an increased aggregation rate. In addition, the oxidized Fc displayed an increased deamidation (at pH 7.4) rate at the Asn 67 and Asn 96 sites, both located on the C_H2 domain, while the deamidation rates of the other residues were not affected. The methionine oxidation resulted in changes in the structure and stability of the Fc, which are primarily localized to the C_H2 domain. These changes can impact the Fc's physical and covalent stability and potentially its biological functions; therefore, it is critical to monitor and control methionine oxidation during manufacturing and storage of protein therapeutics.

Methionine oxidation can play an important role in altering a protein's *in vitro* and *in vivo* stabilities. While the in vivo stability of several proteins upon methionine oxidation has been related to biological functions (*1–4*), the *in vitro* protein stability is critical for the development of protein therapeutics (*5–9*). The mechanism of methionine oxidation by reactive oxygen species has been reviewed recently (*9, 10*). For protein drug products, methionine oxidation can occur during fermentation, purification, formulation, manufacturing, and product storage. Methionine oxidation not only can impact the stability and activity of the protein products but also is a concern for potential immunogenic response (*11*). Therefore, it is essential to characterize the effect of methionine oxidation on the protein drug's structure, stability, and biological activity.

Because the Fc[1] has a long *in vivo* half-life due in part to its ability to interact with the neonatal Fc receptor (FcRn) (*12, 13*), the Fc region of human immunoglobulin G (IgG) has been widely used to construct Fc fusion proteins to afford more effective biological therapeutics with improved serum half-life (*14*). The Fc region is typically comprised of the 227 C-terminal residues of the heavy chain of the human IgG1 (Figure 1A), including the hinge region, the C_H2 and C_H3 domains (*15–17*). It forms a homodimer via covalent disulfide linkages in the hinge region and noncovalent interaction involving the C_H3 domain. There are two intramolecular disulfide bonds per monomer and two intermolecular disulfide bonds linking the two monomers. Each monomer has two methionine residues, Met 33 (Met 252, based on the intact heavy chain sequence) and Met 209

* To whom correspondence should be addressed: Department of Pharmaceutics, Amgen, Inc., One Amgen Center Dr., B2-1-A Thousand Oaks, CA 91320. Phone: (805) 313-5206. Fax: (805) 375-5794. E-mail: liud@amgen.com.

‡ Department of Pharmaceutics, Amgen, Inc.

§ Department of Protein Science, Amgen, Inc.

△ University of California.

[1] Abbreviations: 2D, two-dimensional; 3D, three-dimensional; ACN, acetonitrile; CD, circular dichroism; CH2, constant heavy chain domain 2; CH3, constant heavy chain domain 3; DSC, differential scanning calorimetry; DTT, dithiothreitol; Fc, fragment crystallizable; HPLC, high-pressure liquid chromatography; HSQC, heteronuclear single-quantum correlation; IgG, immunoglobulin G; IPA, 2-propanol; MS, mass spectrometry; NMR, nuclear magnetic resonance spectroscopy; RP, reversed-phase; SASA, solvent accessible surface area; SEC, size-exclusion chromatography; TFA, trifluoroacetic acid.

10.1021/bi702238b CCC: $40.75
Published on Web 04/12/2008

A

```
1   MDKTHTCPPCPAPELLGGPSVFLFPPKPKD  30
31  TLMISRTPEVTCVVVDVSHEDPEVKFNWYV  60
61  DGVEVHNAKTKPREEQYNSTYRVVSVLTVL  90
91  HQDWLNGKEYKCKVSNKALPAPIEKTISKA 120
121 KGQPREPQVYTLPPSRDELTKNQVSLTCLV 150
151 KGFYPSDIAVEWESNGQPENNYKTTPPVLD 180
181 SDGSFFLYSKLTVDKSRWQQGNVFSCSVMH 210
211 EALHNHYTQKSLSLSPGK
```

B

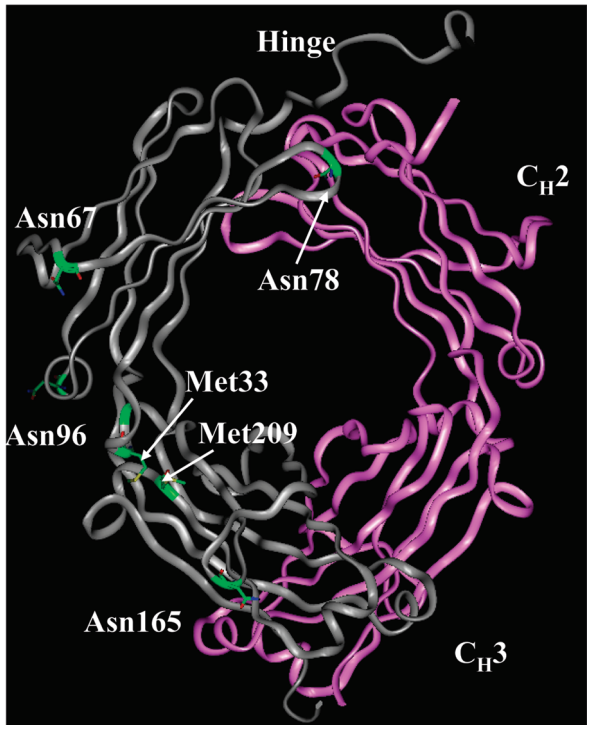

FIGURE 1: (A) Amino acid sequence of human IgG1 Fc expressed in *E. coli*. The residues that undergo covalent degradation are highlighted. (B) Ribbon representation of the Fc region. The crystal structure of human IgG1 (PDB entry 1HZH) was used to prepare the figure.

(Met 428, based on the intact heavy chain sequence) (*18*). Met 33 is located within a short α-helical structure of the C_H2 domain, while Met 209 is in a β-conformation within the C_H3 domain (Figure 1B). Typically, IgG1 Fc and Fc fusion proteins, such as Enbrel, are produced in mammalian cell lines. Alternatively, an *Escherichia coli* expression system can be used to effectively produce Fc and Fc fusion proteins (*19, 20*). The Fc produced using an *E. coli* system is in the form of inclusion bodies which need to be solubilized and refolded. In addition, the *E. coli*-expressed Fc contains an additional methionine residue at the N-terminus due to a cloning artifact, and it is not glycosylated at Asn 78 (equivalent to Asn 297, if using the antibody sequence) due to the lack of this posttranslational modification for *E. coli*.

Methionine oxidation has been reported for several recombinant monoclonal antibodies and Fc fusion proteins developed as protein therapeutics (*21–23*). The methionine residues of the Fc region were found to be susceptible to oxidation during storage (*22*) and upon exposure to the active oxygen species in the formulation (*21*). Recently, Liu et al. (*24, 25*) reported that upon oxidation of methionine residues, the C_H2 domain was more susceptible to protease cleavage, indicating a potential destabilization of the C_H2 domain. However, no detailed structural characterization was presented due to the limitations of their techniques. Here we report our results in a study of methionine oxidation and impact on the structure, thermal stability, and shelf life stabilities of *E. coli*-expressed Fc. Since the sequence and structure of the *E. coli*-produced Fc are nearly identical to the Fc regions in the IgG1 and IgG2 monoclonal antibodies and in the Fc fusion proteins, the results obtained here have broad implications for the development of the Fc-related protein therapeutics.

MATERIALS AND METHODS

Materials. The *E. coli*-produced Fc and Fc mutants used in this study were produced at Amgen (*26*). Briefly, the protein was expressed as an inclusion body. The inclusion body was solubilized and then refolded prior to the purification using chromatography. After the refolding reaction, protein was purified using a protein A affinity column. It was further purified using a fast flow Q column. The chemicals used for HPLC analysis were analytical grade materials. Hydrogen peroxide (H_2O_2) was purchased from Alfa Aesar (Ward Hill, MA) as a 30% solution. Lys-C endoprotease was purchased from Roche Diagnostics (Indianapolis, IN), and trypsin was purchased from Worthington Biochemical Corp. (Lakewood, NJ).

Preparation of Methionine-Oxidized Fc. Methionine-oxidized Fc samples were prepared by mixing aliquots of a 30% H_2O_2 solution with a 10 mg/mL protein solution [10 mM sodium phosphate (pH 7.0) or 10 mM acetate (pH 5.0)]. The final concentration of H_2O_2 obtained was 0.3%. The oxidation reactions were conducted at room temperature; aliquots were taken at the following time points: 40, 140, 240, 400, and 600 min. The samples were then dialyzed extensively with a buffer composed of 10 mM acetate (pH 5.0) at 4 °C to remove H_2O_2. To minimize the additional oxidation during the dialysis, the dialysis buffer was precooled to 4 °C prior to dialysis. In addition, up to three buffer exchanges were carried out to ensure there was no significant amount of hydrogen peroxide left. For the aggregation study, 0.5 mL aliquots of a 2 mg/mL Fc solution from each time point were transferred into 3 cm^3 glass vials; the samples were stored at 45 °C in the dark. For the deamidation study, a hydrogen peroxide treated (600 min) sample and an untreated sample were both exchanged into PBS and stored at 45 °C in the dark.

Lys-C Peptide Map and LC−MS Analysis. A nonreduced Lys-C digestion was performed to analyze all the oxidized Fc samples by the diluting Fc sample into a 0.2 M phosphate buffer (pH 7.5) with 1 M urea and 20 mM hydroxylamine (Sigma, P/N H9876) to a final concentration of 1 mg/mL; typically, a reaction volume of 100 μL was used. The Lys-C enzyme:protein ratio was 1:20. The reaction mixture was incubated at 37 °C for 16 h, and an aliquot of 20% TFA was added to achieve a final TFA concentration of 0.2% to quench the reaction. Digested samples were analyzed using

a reversed-phase HPLC method with an Agilent 1100 HPLC system. The digested samples were chromatographed using a Kromasil C-8 silica column [150 mm × 2.0 mm, 3.5 μm particle size, 100 Å pore size (Phenomenex, catalog no. 00F-4282-B0)]. Separation was achieved with a gradient using two solvents (A, 0.1% TFA in water; B, 0.1% TFA in acetonitrile) at a flow rate of 0.2 mL/min from 0 to 5% B over 5 min, from 5 to 25% B over 10 min, and from 25 to 40% B over 25 min at 50 °C. The gradient was changed to 95% B over 5 min and then continued for an additional 5 min to complete the RP-HPLC run.

Mass spectrometric analysis was carried out on a Waters LCT Premier orthogonal ESI-TOF mass spectrometer. The LCT premier was operated in positive ion mode with W time-of-flight mode and a resolution of 10000. The capillary and cone voltages were set at 3300 and 120 V, respectively. The ion guide one was at 120 V. The desolvation and source temperatures were set at 350 and 100 °C, respectively. All other voltages were optimized to provide maximal signal intensity. Deconvolution of ESI mass spectra was performed using Masslynx MaxEnt 1 software from Waters.

Tryptic Map and LC−MS/MS Analysis. The Fc samples were reduced and alkylated before tryptic digestion using a similar protocol as described previously (*27*). The reduced and alkylated sample was buffer exchanged into a digestion buffer [0.1 M Tris (pH 7.5), 1 M urea, and 20 mM hydroxylamine]. Trypsin was added to yield a final enzyme protein ratio of 1:25 and the mixture incubated at 37 °C for 4 h. The digestion reaction was stopped by lowering the pH using 20% formic acid.

The trypsin digests were separated using a Polaris Ether C18 column (2.0 mm × 250 mm, Varian) maintained at 50 °C. Solvent A consisted of 0.1% aqueous TFA, and solvent B included 90% acetonitrile and 0.085% aqueous TFA. A flow rate of 0.2 mL/min was used to elute the various compounds. A linear gradient from 0 to 50% B was run over 195 min. A Thermo Finnigan Ion Trap mass spectrometer (LCQ DECA) was used in-line with the HPLC system to identify the digestion products. The masses of peptides and their fragments were obtained using a triple-play method that included full scan, followed by zoom and MS/MS scans. A standard off-axis ESI source was used as an atmosphere−vacuum interface. The spray voltage was 5 kV, and the capillary temperature was 250 °C. The MS/MS spectra were obtained using ion trap collision energies of 35%. The percentage of the oxidized peptides was quantified using the UV data for Met 33 and Met 209.

Nonreduced and Reduced SDS−PAGE. A 4 to 20% gradient gel was used for SDS−PAGE analysis of the Fc samples (Invitrogen, Carlsbad, CA). The protein sample was diluted with water to 1 mg/mL and mixed with the 2× gel loading buffer either with DTT (reduced) or without DTT (nonreduced). Then the sample was heated for 10 min at 70 °C prior to loading. A total of 10 μg of protein was loaded. The gel was run with a constant voltage (200 V) and was processed with the SimpleBlue stain solution. Mark 12 (Invitrogen) molecular weight standards were used as a reference for SDS-PAGE analysis.

Circular Dichroism (CD). CD spectra were obtained with a Jasco J-810 spectropolarimeter. The near-UV CD spectra were collected from 310 to 260 nm with a Helma QS cuvette with a path length of 1 cm. The scan speed was 10 nm/min, the response time was 8 seconds, and the bandwidth 1 nm, and an average of five scans was obtained for each sample at 25 °C. The protein concentrations were between 0.7 and 0.8 mg/mL in 0.1 M sodium acetate buffer (pH 5.2). The far-UV CD spectra were collected from 250 to 190 nm with a cuvette with a path length of 0.1 cm. The scan speed was 20 nm/min, the response time was 4 seconds, and the bandwidth 3 nm, and an average of eight scans was obtained for each sample at 25 °C. The protein concentrations were within 0.13−0.14 mg/mL in 10 mM sodium acetate (pH 5.2). Buffer spectra (without protein) were subtracted from the individual sample spectra. A mean residue weight of 112.58 was used to convert ellipticity to mean residue molar ellipticity (MRE).

NMR Spectroscopy. 2D $^{1}H-^{15}N$ HSQC spectra were acquired at 25 °C using a Bruker DRX Advance II 600 MHz NMR spectrometer (Bruker) equipped with an inverse TXI, z-gradient cryogenic probe and on a Varian INOVA 800 MHz NMR spectrometer equipped with a 5 mm triple-resonance probe. The chemical shifts were referenced using 2,2-dimethyl-2-silapentanesulfonic acid (DSS).

The HSQC methionine oxidation experiments were performed using a 5 mg/mL ^{2}H-, ^{15}N-, and ^{13}C-labeled Fc sample in 10 mM sodium acetate buffer (pH 5.0) with 10% deuterium oxide (D_2O). A reference HSQC spectrum was acquired prior to addition of hydrogen peroxide. A 12 μL aliquot of a 30% H_2O_2 solution was added to 0.6 mL of Fc NMR sample to initiate the reaction. Since a higher ratio of hydrogen peroxide to protein (∼1800:1) was used for this experiment, a faster rate of methionine oxidation was anticipated. A short NMR experiment (HSQC) was selected to monitor the spectral change during the oxidation reaction. Sixteen scans were used for each HSQC spectrum; the total experiment time of each spectrum was 39 min. Four HSQC spectra were acquired during the incubation at 25 °C. At the end of the reaction, nearly complete oxidations of Met 33 and Met 209 were expected on the basis of the oxidation rate determined previously. Spectra were processed using NMRPipe (*28*) and analyzed using NMRView (*29*).

Differential Scanning Calorimetry (DSC). DSC was carried out using a MicroCal VP-capillary DSC instrument. The protein sample was dialyzed extensively into 10 mM acetate buffer (pH 5.0). Protein concentrations of ∼0.25 mg/mL were used for the experiments. A scan rate of 1.67 °C/min was used for all the experiments. Data were processed using Origin 7 supplied by MicroCal. Melting temperatures (T_m) were obtained by fitting the DSC data to a nonlinear regression routine provided with Origin.

Size-Exclusion Chromatography (SEC). SEC was performed using an Agilent 1100 liquid chromatography system equipped with ChemStation. A TSK-GEL $G3000W_{XL}$ column (Tosoh Biosciences) was employed for chromatographic separation using 50 mM sodium phosphate (pH 6.5), 300 mM sodium perchlorate, and 10% 2-propanol as the mobile phase. The protein was monitored using UV detection at 214 and 280 nm.

RESULTS

Analysis of the Methionine-Oxidized Fc and Oxidation Reaction Kinetics. To study the relative oxidation rate of each methionine residue and to obtain Fc samples with

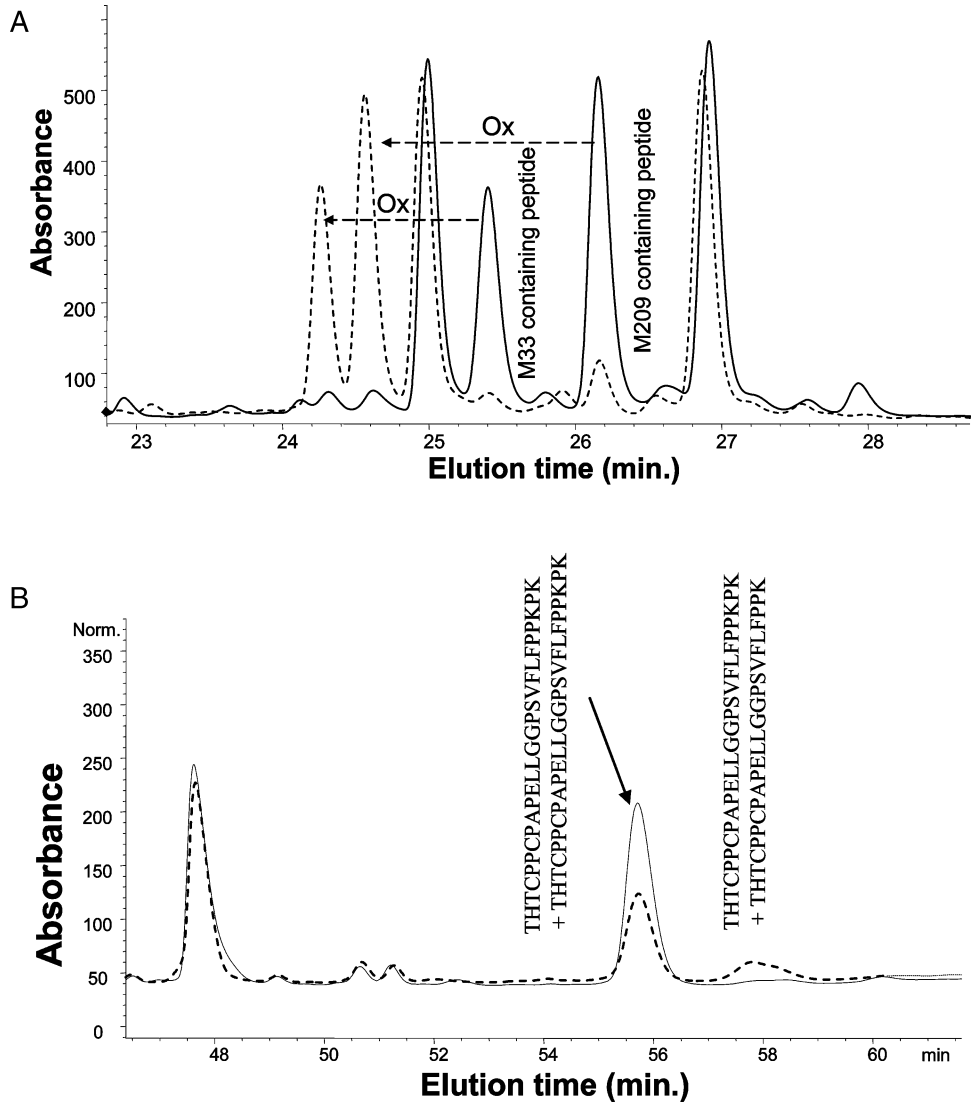

FIGURE 2: Reversed-phase HPLC chromatogram of the nonreduced Lys-C map of Met-ox-Fc (t = 400 min, dashed line) and the untreated Fc (solid line). Only the peptide portions corresponding to the regions of the two intrachain disulfide bonds (Cys 42/Cys 102 and Cys 148/Cys 206) (A) and of the interchain hinge region disulfide bonds (B) are shown.

different percentages of methionine oxidation, the oxidation reaction was performed by incubating the Fc protein in the presence of hydrogen peroxide. A protein concentration of 0.2 mM was used, while the hydrogen peroxide concentration was at 90 mM giving a H_2O_2:Fc mole ratio of ~450. A nonreduced Lys-C map method was used to analyze Fc samples from all the time points to detect the potential changes in disulfide bond structure as a result of the oxidation reaction (Figure 2), and data from t = 0 and t = 400 min time points are shown in Figure 2. Peptide assignments were achieved on the basis of their calculated peptide mass. Two peptides, Asp 30−Lys 55(Cys 42)/Cys 102−Lys 103(Cys 102) and Asn 142−Lys 151(Cys 148)/Ser 196−Lys 220(Cys 206) (the slash representing one disulfide bond), which contain the intrachain disulfide bonds within the Fc region, eluted at 25.4 and 26.2 min, respectively (Figure 2A). After the treatment with H_2O_2, the elution times of these peptides were shifted to 24.2 and 24.6 min, respectively. The mass of the peptides was the mass of the native peptides plus 16 Da, consistent with the formation of the methionine sulfoxide. No additional peaks corresponding to these two peptides were identified. The peptide peak corresponding to the hinge region with two interchain disulfide bonds, Thr 4−Lys 29// Thr 4−Lys 29 (two slashes representing two disulfide bonds), eluted at 55.8 min with a mass of 5453.6 Da (Figure 2B). There is an additional lysine residue (Lys 27) within this peptide. The peak intensity of this peptide was lowered as the time of hydrogen peroxide treatment (i.e., extent of methionine oxidation) increased, while a peak eluting at 58.0 min exhibited increased intensity. The mass of this peak was measured as 5228.7 Da and was identified as Thr 4−Lys 29//Thr 4−Lys 27, an alternative Lys-C cleavage product of Thr 4−Lys 29//Thr 4−Lys 29 (see Figure 1A for the sequence details). Therefore, the retention time changes of these disulfide-containing peptides were due to the methionine oxidation and change in the cleavage pattern, and they are not due to any other chemical modification of the disulfide bond upon treatment with H_2O_2. To further confirm that no chemical modification other than methionine oxidation occurred during the incubation with H_2O_2, a reduced and alkylated tryptic map method was used to analyze the H_2O_2-treated samples. Chemical modifications other than methionine oxidation of Met 1, Met 33, and Met 209 were not detected. On the

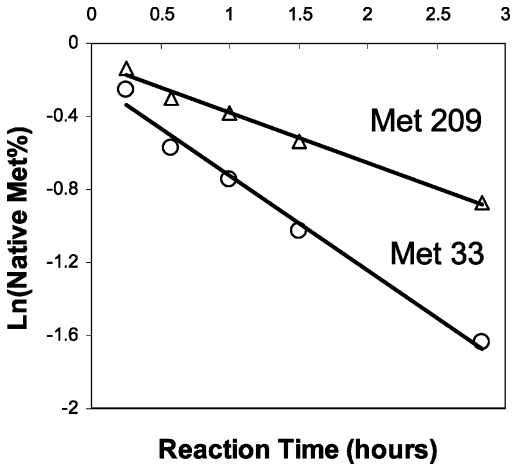

FIGURE 3: Kinetics of methionine oxidation. Rates of methionine residues (triangle for Met 209 and circle for Met 33) shown to be oxidized can be determined from the slopes of the linear fits through the data.

basis of the analysis given above, we conclude that methionine oxidation was the only detectable chemical change as a result of treatment with H_2O_2.

The percentage of methionine-oxidized peptide was determined using a reduced and alkylated tryptic peptide mapping method. Figure 3 shows the time course of the oxidation reaction at room temperature for each methionine residue. The kinetic data were fitted to an exponential decay equation to obtain the oxidation rate constants of each methionine residue. The good fit to the data ($R^2 > 0.99$) indicated the oxidation reaction was a pseudo-first-order reaction which is consistent with the literature reports (*9*). Met 33 is the faster methionine to be oxidized with a rate constant of -0.53 h^{-1}, while the rate constant of Met 209 oxidation was determined to be -0.27 h^{-1}.

Impact of Methionine Oxidation on Fc's Structure. The effects of H_2O_2 oxidation on secondary and tertiary structure of the Fc were evaluated by far-UV and near-UV CD, respectively. Figure 4 shows the near- and far-UV CD spectra of the Fc and Met-ox-Fc ($t = 400$ min) samples. The far-UV CD spectrum of Fc (Figure 4A) exhibits a negative band near 218 nm and a positive band around 203 nm, indicating Fc is a β-sheet protein, consistent with the crystal structure of the Fc fragment (*30*) and the intact antibody (*17*). The second negative band near 230 nm is due to the significant contributions from aromatic amino acid residue side chains, especially in a low-α-helix content protein (*31–33*). After H_2O_2 oxidation treatment, the overall far-UV CD spectra of Met-ox-Fc show a small change, indicating that the majority of the secondary structures were largely retained, but there are some perturbations on the overall structure. The MRE value at 218 nm decreased by ~10% for the Met-ox-Fc samples, indicating a small but detectable change in its secondary structure. An increase in positive ellipticity was observed for the Met-ox-Fc samples in the near-UV spectra compared to the native Fc (Figure 4B). Since the near-UV spectra reflect the tertiary structure and the environments of aromatic amino acid residues and disulfide bonds (*34*), the near-UV CD spectral change further supports the notion that oxidation of the methionine residues also resulted in a perturbation of the Fc's tertiary structure.

Methionine Oxidation of Fc Characterized by $^1H-^{15}N$ HSQC. To obtain more detailed information about Fc structural changes as a result of methionine oxidation, 2D $^1H-^{15}N$ HSQC was used to monitor the oxidation reaction. Since the peak position and peak shape in a HSQC spectrum are related to the protein structure and dynamics, HSQC is widely used to monitor protein structural and dynamic changes accompanied by the physical and chemical processes on a per-residue basis. Figure 5A shows the HSQC spectra measured before and after the treatment of hydrogen peroxide. The sequence specific resonance assignments are labeled. Note that the assignments were achieved by analyzing the 3D triple-resonance experiments and will be reported elsewhere (*35*). After the addition of hydrogen peroxide, the majority of the peaks in the spectrum were identified with the same spectral properties (peak position and line width), indicating the oxidized protein is still largely folded; however, several peaks exhibited significant changes in peak intensity and/or chemical shift (Figure 5A,B). Residues that experienced significant chemical shift changes are Thr 4 and Thr 6 of the hinge region, Ser 35, Arg 36, Val 89, Gln 92, and Trp 94 of the C_H2 domain, Gly 122 and Gln 123 of the linker region between the two domains, and Phe 153, Asp 157, Ala 159, Glu 161, Trp 162, Lys 190, Ala 212, and Gln 219 of the C_H3 domain (Figure 5B). Moreover, several peaks in the HSQC spectrum, such as Lys 29, Asp 30, Thr 31, Ile 32, and Met 33 of the C_H2 domain, Ala 120 of the linker region, and Ser 207, Met 209, His 210, His 216, and Tyr 217 of the C_H3 domain, became weaker in intensity as the oxidation reaction went on; at the end of the reaction, these peaks disappeared completely. There are several new peaks that appeared at the end of the oxidation reaction (Figure 5A); interestingly, the number of new peaks that can be identified is smaller than the number of peaks that disappeared. This could be due to spectral overlaps and/or peak broadening as a result of increased protein dynamics and conformational exchange after methionine oxidation.

Impact on Fc's Thermal Stability. Differential scanning calorimetry (DSC) was used to characterize the thermal stability of the native and methionine oxidized *E. coli*-expressed Fc samples. Two distinguished thermal transitions were observed in the thermogram of the Fc (Figure 6A). The first temperature transition is attributed to the thermal unfolding of the C_H2 domain, while the second transition is due to unfolding of the C_H3 domain (*36, 37*). The T_m values of C_H2 and C_H3 domains for the untreated sample are 59.8 and 82.8 °C, respectively. It is worth noting that the C_H2 domain of the native Fc is largely reversible when the temperature of the DSC experiment does not exceed 75 °C (i.e., the C_H3 domain is not thermally denatured; D. Liu et al., unpublished data). This is qualitatively consistent with the literature report for deglycosylated Fc (*37*), although the T_m value for the C_H2 domain is 5 °C lower. The difference in thermal stability may be due to the difference in the solution conditions (i.e., pH, additives) between this study and the previous study (7.4 vs 5.0), since the thermal stability of the C_H2 domain is sensitive to the pH. The T_m values for the C_H2 and C_H3 domains were determined for the Fc samples containing different percentages of oxidized Met 33 and Met 209 (Figure 6B). Although both the C_H2 and C_H3 domains contain one methionine residue which can be oxidized, a rather large shift in T_m was observed for the C_H2

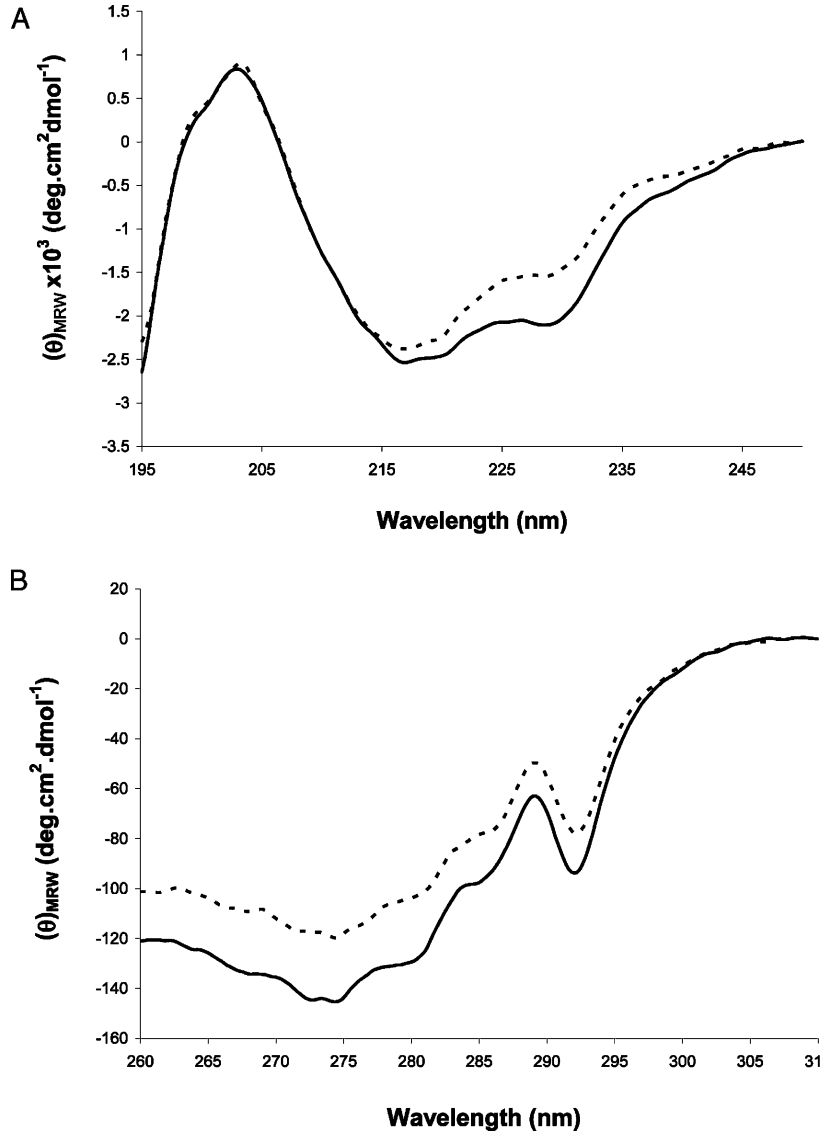

FIGURE 4: (A) Far-UV CD spectra of *E. coli*-expressed human IgG1 Fc (solid line) and Met-ox-Fc (dotted line). The samples consisted of ~0.13 mg/mL protein in 10 mM sodium acetate (pH 5.2). (B) Near-UV CD spectra of *E. coli*-expressed human IgG1 Fc (solid line) and Met-ox-Fc (dotted line). The protein concentrations were 0.7−0.8 mg/mL. All data were acquired at 25 °C. The percentages of methionine (Met 33 and Met 209) oxidation determined by the tryptic map method are 8.9 and 5.5% (t = 0) and 100 and 98.6% (t = 600 min), respectively.

domain after oxidation and a small change in the T_m was observed for the C_H3 domain. Figure 6B shows the T_m value changes as a function of the total percent of oxidized Met 33 and Met 209. The good linearity (R^2 = 0.96) observed for the fitting indicated that oxidation of both methionine residues is likely contributing to the decrease in thermal stability.

Thermal Stability of Fc Mutants upon Methionine Oxidation. To further investigate the contributions of Met 33 and Met 209 to the destabilization of the C_H2 domain upon oxidation, we obtained two mutants from a previous study (*26*). The first mutant, Fc-A2, has two mutation sites, Met 33 to a Leu residue and Thr 37 to a Phe residue; the second mutant, Fc-A8, has four mutation sites: Gln 167 to an Arg residue, Met 209 to a Leu residue, Asn 215 to a His residue, and Tyr217 to a Leu residue. The additional mutations other than methionine residues were previously designed for improving FcRn−Fc interaction. The mutants are not ideal but can be used for evaluating the contribution from each methionine oxidation to the stability changes in the Fc region. Notice that Fc-A2 mutations are only on the C_H2 domain while the changes of Fc-A8 are all within the C_H3 domain. The mutants were treated with hydrogen peroxide to generate methionine-oxidized samples. Due to the limited sample quantities, only two time points were taken during the treatment. The percentage of methionine oxidation was determined using the tryptic map method.

The C_H2 domain DSC results of the oxidized mutants are summarized in Figure 6C. For the untreated samples, the T_m values of C_H2 and C_H3 domains were determined to be 54.8 and 82.0 °C for Fc-A2 and 56.6 and 77.0 °C for Fc-A8, respectively. Mutations Met33Leu and Thr35Phe on the C_H2 domain (Fc-A2) lowered the T_m of the C_H2 domain by ~5 °C while having little impact on the stability of the C_H3 domain. The mutations on the C_H3 domain (Fc-A8), however, lowered the T_m values of both the C_H2 (~3 °C) domain and the C_H3 (~5 °C) domain. The C_H2 domain is much less stable than the C_H3 domain as indicated by their correspond-

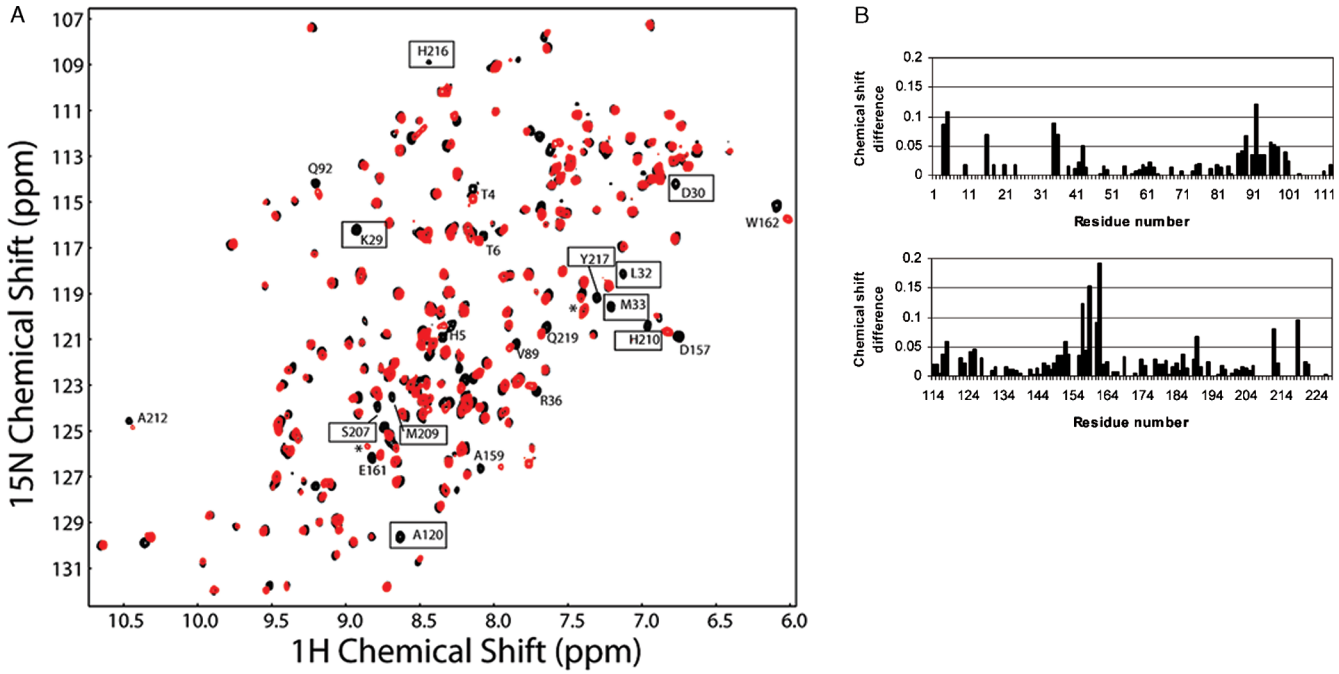

FIGURE 5: (A) $^{1}H-^{15}N$ HSQC spectra acquired at 800 MHz. Spectra acquired prior to the addition of hydrogen peroxide (black) and 3 h (red) after the addition of the hydrogen peroxide are shown. Only the selected peaks are labeled with their assignments. The assignments of peaks that disappeared at the end of oxidation are boxed. (B) Weighted average chemical shift differences (calculated as $|\delta^{1}_{H,t=0} - \delta^{1}_{H,t=3h}| + |\delta^{15}_{N,t=0} - \delta^{15}_{N,t=3h}|$, where δ represents the chemical shift value in parts per million) for the Fc before and after the oxidation reaction. The graphs show residue specific differences between the chemical shift before and 3 h after the addition of H_2O_2.

ing melting temperatures; therefore, even the amino acid substitutions on the C_H3 domain can affect the C_H2 stability. Interestingly, oxidation of methionine residues of both mutants lowered the melting temperature of the C_H2 domain, although a different slope was obtained for Fc-A2 and Fc-A8 when the changes of the C_H2 domain T_m value were plotted against the percent of methionine oxidation (Figure 6C). Compared with that of the wild-type Fc, the slope obtained for Fc-A8 (Met 209 not present, only Met 33 oxidized) is -4.97 ± 0.43, which is slightly less than that of the wild-type Fc (-6.30 ± 0.93), while the slope values of Fc-A2 (Met 33 mutated, only Met 209 oxidized) is -9.71 ± 1.32, which is almost twice the value of Fc-A8 and 1.5 times of the value of the wild-type Fc.

Impact of Methionine Oxidation on Aggregation. The physical stability of the Fc and oxidized Fc samples was evaluated by size-exclusion chromatography. Figure 7A shows the aggregation kinetics of these samples. The total aggregate formation for the untreated Fc sample (contains ~13% oxidized Met 33 and Met 209) was less than 1% after incubation at 45 °C for up to 28 days. In contrast, ~50% aggregate formation was observed during the same period for the Met-ox-Fc sample containing nearly completely oxidized Met 33 and Met 209. Reduced and nonreduced SDS−PAGE methods were used to analyze the stability of the samples. Interestingly, the aggregates observed using SEC, including dimer and larger aggregates, were largely not observed in the nonreduced SDS−PAGE (Figure 7B). The faint high-molecule bands presented in the SDS−PAGE gel are only a small fraction of the total aggregates as detected by SEC. This indicates the aggregates observed using the SEC method are largely noncovalent in nature.

Impact on Fc Deamidation Rate. To determine the impact of methionine oxidation on the covalent stability of the Fc, such as deamidation rate, untreated and fully methionine-oxidized Fc samples were buffer exchanged into PBS (pH 7.4) and stored at 45 °C for 25 days. The covalent degradations were quantified using the tryptic peptide map and LC−MS method (*38*).

The main covalent degradation of the Fc in PBS (pH 7.4) was deamidation of asparagine residues (*38*). Residues Asn 67, Asn 78, Asn 96, and Asn 165 were identified previously as the asparagine residues that can undergo deamidation under heat-stressed conditions. Among these residues, Asn 78 was found to be the most unstable residue, while Asn 96 was deamidated only slightly (*38*). These chemical modifications are evident from the comparison of the tryptic maps of the Fc samples formulated in PBS before and after storage at 45 °C for 25 days. Nearly equal amounts (~60%) of Asn 78 deamidated after storage for both the nonoxidized and Met-ox-Fc samples (Figure 8A). This was also true for the Asn 165-containing peptide fragment. In contrast, the deamidation rates were very different for Asn 96 of Met-ox-Fc in comparison with those of the untreated Fc sample. A 23% deamidated Asn 96 was found for the nonoxidized Fc after the incubation at 45 °C, while a nearly 2-fold increase (67%) in deamidated Asn 96 was observed for the Met-ox-Fc (Figure 8B). The deamidation of the Asn 67 is also faster in the Met-ox-Fc (data not shown). In short, the methionine oxidation of the Fc has led to increases in levels of deamidation for several residues located on the C_H2 domain.

DISCUSSION

Kinetics of Methionine Oxidation. The Fc region of human IgG1 has two domains, namely, the C_H2 domain and C_H3

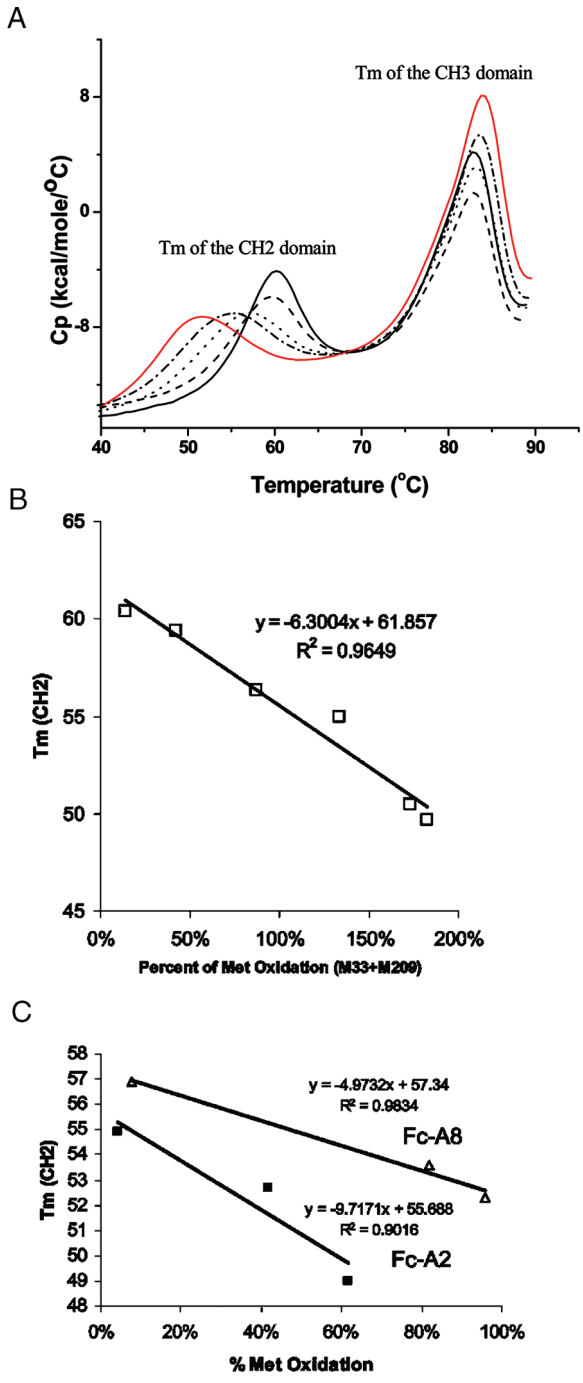

FIGURE 6: (A) Thermograms of *E. coli*-expressed human IgG1 Fc. The percentages of methionine (Met 33 and Met 209) oxidations determined by the tryptic map method for samples used for this study are 8.9 and 5.5% ($t = 0$, solid line), 26.8 and 15.3% ($t = 40$ min, dashed line), 53.0 and 34.1% ($t = 140$ min, dotted line), 76.7 and 56.90% ($t = 240$ min, dashed and dotted line), and 92.40 and 80.50% ($t = 400$ min, solid red line), respectively. (B) Correlation of total methionine oxidation (percent of oxidized Met 33 and Met 209) of Fc with the melting temperature changes of the C_H2 domain. (C) Correlation of combined methionine oxidation for Fc-A2 [M33L/T37F mutant (■)] and Fc-A8 [Q167R/M209L/N215H/Y217L mutant (△)] with the melting temperatures of the C_H2 domain.

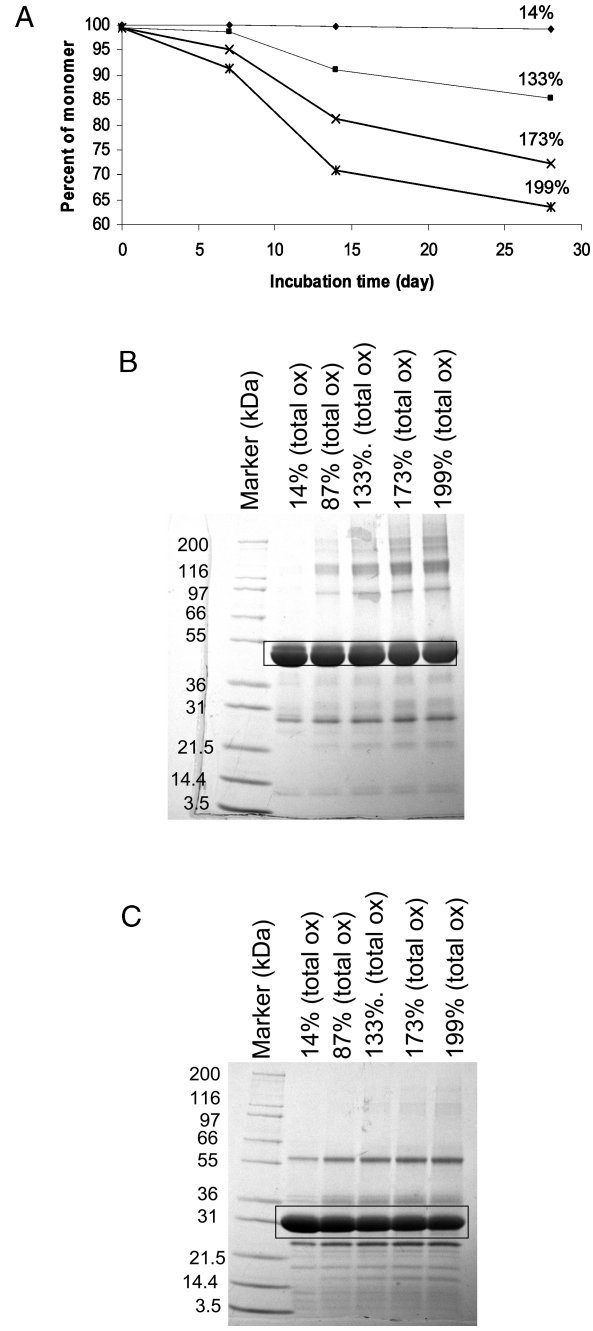

FIGURE 7: Physical stability of Met-ox-Fc analyzed using SEC and SDS−PAGE. (A) SEC results of the Fc samples showing an increased loss of monomer that corresponds to the extent of methionine oxidation. The total percentage of Met 33 and Met 209 oxidation for each sample is labeled. (B) Nonreduced and (C) reduced SDS−PAGE of the methionine-oxidized Fc after incubation for 4 weeks at 45 °C. The percentages of the total methionine (Met 33 and Met 209) oxidations are labeled. The boxed band is the Fc (51.4 kDa).

domain (Figure 1). Each domain contains one methionine residue, Met 33 located on the C_H2 domain and Met 209 located on the C_H3 domain. Although the sequences of the C_H2 and C_H3 domains are nearly 30% similar, the two methionine residues are not structurally equivalent. The Met 33 residue is located within a short helical structure formed by residues Lys 29−Met 33 (Figures 1B and 9B). This helix is packed with the core structure of the C_H2 domain mainly via nonhydrophobic interactions. The Met 209 residue is within a β-strand formed by Val 203−His 210 in the C_H3 domain. Interestingly, both methionine residues are located within the interface of the C_H2 and C_H3 domains. The helix which contains Met 33 is interacting with the C_H3 domain via electrostatic interaction involving Lys 29 and Glu 161 and via hydrophobic interaction involving Met 33 and Met 209. Specifically, the side chains of

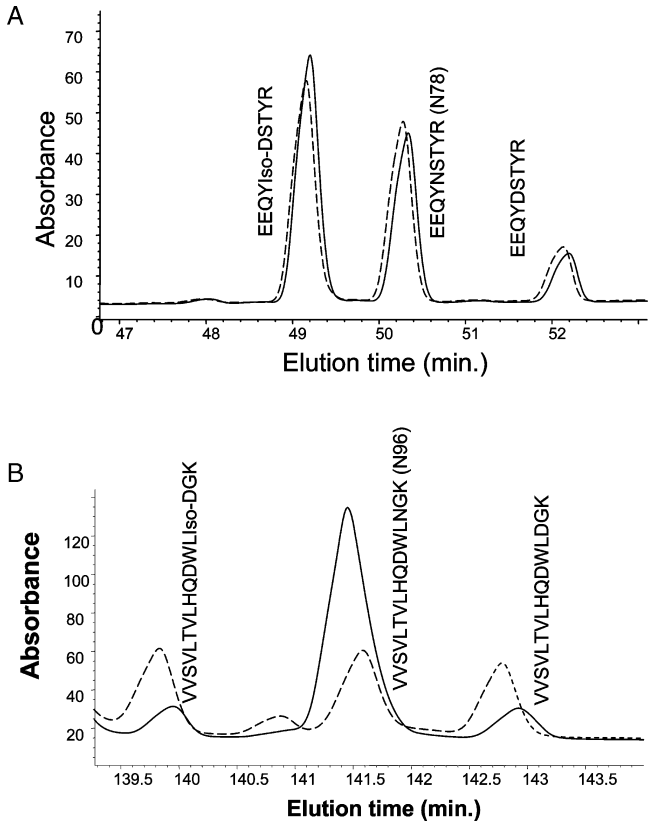

FIGURE 8: Covalent stability changes as a result of methionine oxidation. Overlays of representative regions from RP-HPLC chromatograms of tryptic maps for the Met-ox-Fc (dashed line) and the untreated Fc (solid line): (A) EEQYNSTYR (Asn 78) peptide and (B) VVSVLTVLHQDWLNGK (Asn 96) peptide. Deamidation products are labeled. Both samples were formulated in PBS and stored at 45 °C for 25 days.

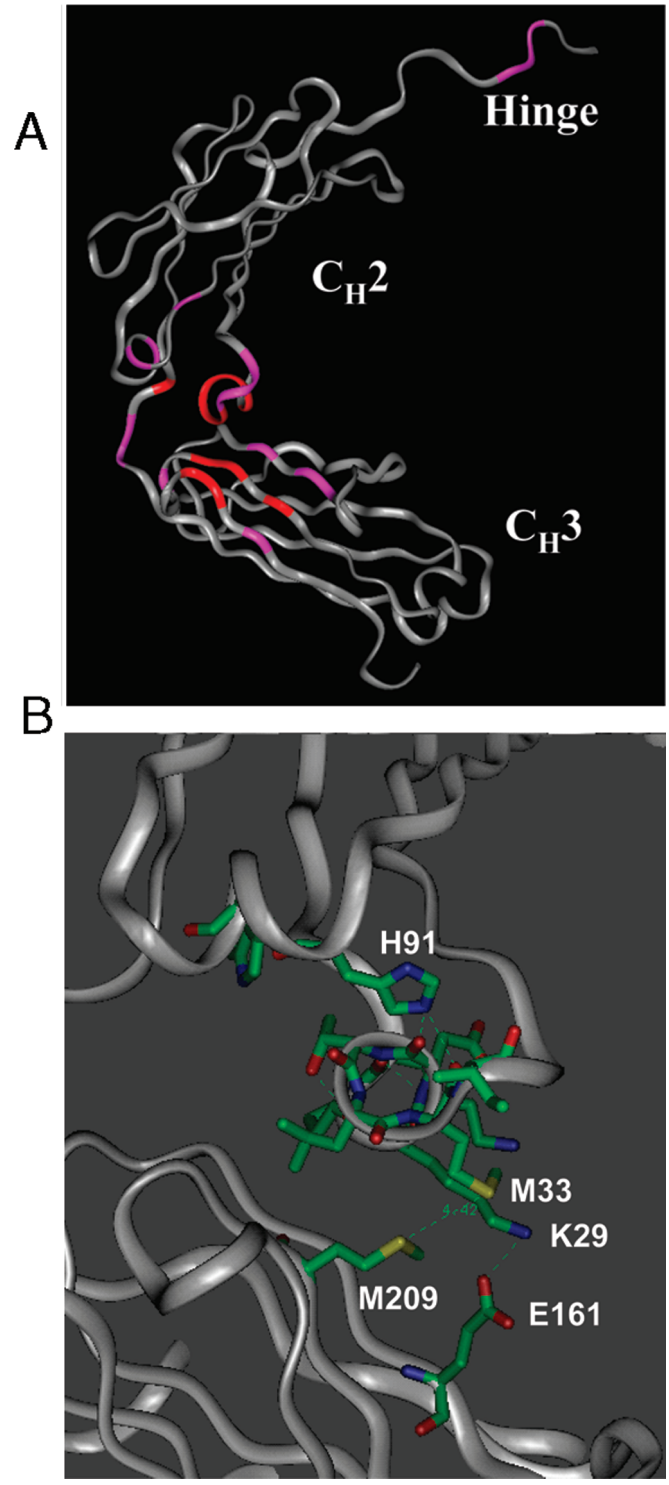

FIGURE 9: (A) Mapping of the chemical shift perturbations of the Fc due to methionine oxidation on the structure of the Fc region. A backbone ribbon representation of the Fc structure with residues that experienced chemical shift changes due to oxidation highlighted in magenta and residues that experienced complete intensity loss highlighted in red. (B) Structure of the Lys 29−Met 33 helix and interactions between the C_H2 and C_H3 domains. A crystal structure of human IgG1 (PDB entry 1HZH) was used for this illustration.

two methionine residues are in a direct contact with each other, the distance between the sulfur atoms of Met 33 and Met 209 being 4 Å, based on the crystal structure of human IgG1. The solvent accessible surface areas (SASAs) of Met 33 and Met 209 calculated using Insight II (Accelrys, San Diego, CA) are 25% and 5%, respectively. The SASA for the side chain sulfur atom was calculated to be 62% and 4% for Met 33 and Met 209, respectively. The oxidation rate for Met 33 was faster than that of Met 209. The SASA data are qualitatively consistent with the order of the reaction rate; however, the rather small difference in the reaction rate constants of Met 33 and Met 209 (2 fold) does not reflect the rather large difference between the solvent accessible surface areas (5-fold) of Met 33 and Met 209. This is likely due to the inaccurate determination of SASA based on the crystal structure of a protein as previously reported (*39*), due to potential structural differences between the crystal structure and solution structure and due to the protein dynamics of the Fc. This also shows that SASA may not be an accurate predictor of the relative reactivity of methionine residues. Further research is needed to accurately predict methionine oxidation in proteins.

Structural Consequence of Methionine Oxidation. There are several reports about the identification of the methionine oxidation in the Fc region of recombinant human IgG1 antibodies (*24, 25*). However there is only one reported attempt to evaluate the impact of methionine oxidation on the stability of an antibody using limited proteolysis (*25*). On the basis of the increased susceptibility of proteolytic cleavage after methionine oxidation, it was suggested that perhaps methionine oxidation resulted in a conformational change in the C_H2 domain of IgG1 Fc (*25*). The primary method used in the study was proteolysis followed by LC−MS analysis; no biophysical method was used for the

study. This report did not provide detailed structural evidence of conformational and stability changes.

The advantage of using the *E. coli*-expressed Fc is that the isotope-labeled protein can be produced for structural studies using solution NMR techniques. The structure of the *E. coli*-produced Fc is nearly identical to that of the CHO cell-expressed Fc based on the extensive characterization studies (details will be published elsewhere). The CD and NMR results have shown that the methionine oxidation has resulted in a significant structure change in the Fc region. While the CD data showed the global secondary and tertiary structure changes, NMR data offered great details about the structural impact of methionine oxidation on the Fc region. The most dramatic change in the HSQC spectra resulting from methionine oxidation is that the resonances of some residues disappeared at the end of the oxidation reaction; they include residues Lys 29, Asp 30, Thr 31, Leu 32, and Met 33 which are within the Met 33-containing helix on the C_H2 domain, Ala 120 which is in the linker region between the C_H2 and C_H3 domains, and Ser 207, Met 209, His 210, His 216, and Tyr 217 of the C_H3 domain (Figure 5A). In addition, the residues that experienced the largest chemical shift changes during oxidation were Gln 92, Trp 94, Asp 157, Ala 159, Glu 161, and Trp 162 (Figure 5B). Almost all of these residues, except Gln 92, Trp 94, and Ala 120, are located in the proximity of the methionine residues and are part of the C_H2 and C_H3 domain interface. Since the modification by hydrogen peroxide is to add an oxygen atom to the side chain of either methionine residue (Met 33 and Met 209), the large changes in backbone amide chemical shift and intensity observed are likely due to the changes in the chemical and electronic environment surrounding each side chain and conformational alternations in the local structure. The residues that disappeared in the HSQC spectrum at the greatest oxidation level likely have very different chemical shift values. Indeed, new peaks have appeared in the HSQC spectra acquired after oxidation for 3 h (Figure 5A). The identities of the new peaks will be determined in future studies. The change observed for Ala 120 is significant; since it is located between the C_H2 and C_H3 domain, this implies that the oxidation has led to a change in the domain−domain interaction. Interestingly, residues Thr 4, His 5, and Thr 6 at the hinge region also exhibited chemical shift changes during the oxidation reaction. This may be due to the effect of the Met 1 oxidation on the local electronic environment and may have little implication concerning the Fc structure and stability in the vicinity of Met 33 and Met 209 since it is far removed and absent in the native Fc sequence (or antibody sequence). Overall, these changes confirm potential structural perturbations caused by oxidation of Met 33 and Met 209 as detected by CD. All the residues described above are mapped to the crystal structure of the human Fc (Figure 9A). While many of the residues are near the sites of the chemical modification, the regions away from the modification sites are also clearly affected. For example, residues Gln 92 and Trp 94 on the C_H2 domain displayed significant chemical shift change (Figure 5A and 5B), indicating methionine oxidation perturbed structures more globally for this domain. These changes can be explained by the crystal structure of the Fc.

In the crystal structure (Figures 1B and 9B), Met 33 is located at the end of a short helical structure formed by residues Lys 29−Met 33 ($K^{29}DTLM^{33}$). This short helix is packed against both the C_H2 and C_H3 domain structures. His 91 from the C_H2 domain formed hydrogen bond interactions with its side chain nitrogen atom (NE2) and the backbone oxygen atoms of Asp 30 and Met 33 of the helix (Figure 9B). Meanwhile, Lys 29 formed a hydrogen bond with Glu 161 of the C_H3 domain. The side chains of Met 33 and Met 209 are tightly packed against each other; therefore, addition of oxygen to Met 33 and/or Met 209 resulting from methionine oxidation can generate unfavorable repulsions between the side chains of the two methionine residues. Such interactions can negatively affect the specific hydrophobic and hydrogen bond interactions which are critical for the stability of the Lys 29−Met 33 helix and for the specific interactions between the C_H2 and C_H3 domains. The conformations of the residues involved in the side chain interactions with Met 209 on the C_H3 domain, such as Trp 162, Ser 207, His 210, and Tyr 219, are affected similarly. The affected residues even farther from the oxidation sites can be due to electronic environmental or conformational changes extended from the site of the modification. A determination of the structure of the oxidized Fc using X-ray crystallography is required to provide the structural basis of the conformational change and is currently a work in progress.

Another interesting point of discussion is the effect of glycosylation on the rate of methionine oxidation and on the stability change as a result of methionine oxidation. Krapp et al. reported a structural analysis of human IgG1 Fc with different glycoforms based on X-ray crystallographic data (*30*). While a clear correlation between glycosylation and structural integrity was revealed, the structural changes as a consequence of glycosylation pattern were limited to the local conformation near the site of glycosylation. Little conformational change was observed in the interface region between the C_H2 and C_H3 domains. This was confirmed by a subsequent NMR study of solution structure of the Fc with various glycoforms, including the deglycosylated Fc (*40*). Since there is little difference in protein structure near the methionine residues between glycosylated and deglycosylated Fc, it is our speculation that glycosylation at Asn 78 may have a minimal impact on the rate of methionine oxidations at the C_H2−C_H3 domain interface. However, the impact of methionine oxidation on the structure of the Fc will likely be similar for the Fc with different glycoforms. The change in protein stability due to methionine oxidation is expected to be similar as well. This has been confirmed by DSC results for the glycosylated Fc with and without methionine oxidation (data not shown). Since the T_m of the C_H2 domain of glycosylated Fc is 5 °C higher than that of the deglycosylated Fc (*37*), the methionine-oxidized glycoslyated Fc is also more thermally stable than the methionine-oxidized deglycosylated Fc. On the basis of the analysis described above, methionine oxidation will have a smaller impact on the shelf life stability (i.e., aggregation and deamidation) of the glycosylated Fc, which is common for CHO cell-derived Fc-containing proteins, such as monoclonal antibodies.

Destabilization of the C_H2 Domain. The structural data show that both the C_H2 and C_H3 domains are affected by oxidation; however, the DSC results showed that the C_H2 domain stability is more significantly perturbed than that of the C_H3 domain. As discussed above, introducing an extra oxygen atom to each sulfur atom as a result of methionine oxidation

can potentially generate a repulsive interaction between the side chains of Met 33 and Met 209 which destabilizes the native state conformation; therefore, this leads to a lower overall conformational stability. Although both the C_H2 and C_H3 domain structures are perturbed, the destabilization effect is mainly on the C_H2 domain, since only the C_H2 domain melting temperature was affected significantly. It is worth noting that although the C_H2 and C_H3 domains are Ig folds that are ~20% identical and ~30% similar in sequence, the thermal stabilities are quite different. The T_m value of the C_H3 domain is nearly 20 °C higher than that of the C_H2 domain. This may be partly due to the formation of the homodimer involving the C_H3 domain. Since the C_H2 domain is intrinsically less stable, it is more sensitive to structural perturbations and destabilization effects afforded by methionine oxidation.

It is interesting that the total percentage of the oxidation for the two methionine residues correlates with the decrease in the C_H2 domain's melting temperature. Such effects imply that both methionine oxidations are contributing to the destabilizing effect. The results from the DSC study using Fc-A2 and Fc-A8 mutants confirmed that indeed oxidation of both Met 33 and Met 209 can destabilize the C_H2 domain. Furthermore, the oxidation of Met 209 may have contributed more to the destabilization effect. This is not surprising since Met 209 is nearly completely buried with SASA values of 5% and is intimately involved in the domain−domain interactions; therefore, it is more critical for maintaining the stability of the Fc in comparison with Met 33. The destabilization of protein structure and stability due to methionine oxidation has been reported for several proteins. In the case of staphylococcal nuclease (*41*), methionine oxidation of the wild-type protein led to a loss of ~4 kcal/mol in $\Delta G_{unfolding}$. A NMR study revealed that the methionine oxidation of residue 388 of thrombomodulin resulted in a significant structural change which led to inactivation of the protein (*42*). Methionine oxidation of monomeirc repressor resulted in a drastic destabilization of the native state structure and enabled protein denaturation under nondenaturing buffer conditions (*43*). The methionine-oxidized Fc largely retained its native conformation, and the impact was limited to the interface between the C_H2 and C_H3 domains.

Interplay between Covalent and Physical Degradations. The thermal stability and structural study results showed that the oxidation of Met 33 and Met 209 resulted in a significant change in the structure and stability of the C_H2 domain. This has important implications in the product shelf life stability studies of Fc-containing protein therapeutics. As shown in the aggregation study, the rate of aggregation is much higher for the oxidized Fc than that of the native Fc. The aggregation behavior correlated with the decreased T_m values which indicated the thermal stability of the samples. The observed physical instability is consistent with the thermal stability and structural changes of the methionine-oxidized Fc. An increased level of methionine oxidation as a result of hydrogen peroxide treatment led to a decreased thermal stability of the C_H2 domain as indicated by the corresponding melting temperature shifts. As the melting temperature of the C_H2 domain was lowered from 60 to 49 °C (with an increase in the level of oxidation), the partially unfolded C_H2 domain becomes increasingly populated and proves to aggregate under 45 °C storage conditions. The increase in the level of the partially unfolded Fc incubated at 45 °C likely resulted in an increased level of noncovalent aggregate formation. Since only the C_H2 domain is partially unfolded, this also implies that the structurally altered C_H2 domain is likely involved in the aggregation pathway.

In addition to physical stability, methionine oxidation has also led to an increase in the deamidation rate of asparagine residues, Asn 67 and Asn 96, both located on the C_H2 domain. This covalent stability change as a result of methionine oxidation is consistent with the notion that methionine oxidation destabilizes the C_H2 domain in such a way to augment the deamidation reaction. Since the deamidation rate is determined in part by the structure and stability of the protein (*44*), the change in covalent degradation rates of Asn 96 and Asn 67 upon methionine oxidation indicates that there are substantial structure and stability differences for the regions surrounding these two asparagine residues before and after methionine oxidation. Since these amino acids are located within the C_H2 domain, and the Asn 96 residue is located in the proximity of the helical structure involving Met 33, it seems plausible that the dramatic increase in the deamidation rate of Asn 96 is consistent with a structural change involving this region and oxidation of Met 33. This is supported by the NMR HSQC data in which changes in the chemical shift values for Gln 92, Trp 94, and several other residues nearby were observed (as discussed above). These data further suggest that methionine oxidation impacts the structure and covalent stability of the C_H2 domain.

CONCLUSION

Methionine oxidation is a concern for the development of protein therapeutics. In this study, methionine oxidation has been shown to affect the structure and stability of the *E. coli*-expressed human IgG1 Fc protein. Met 33 is more readily oxidized than Met 209. Oxidation of Met 33 and Met 209 resulted in a detectable structural change as demonstrated by the far-UV and near-UV CD data. The structural regions affected by methionine oxidation were mapped using $^1H-^{15}N$ HSQC; they are located on both the C_H2 and C_H3 domains. Such structural perturbations as a result of methionine oxidation have a destabilizing effect on the Fc's thermal stability. The melting temperature of the C_H2 domain is reduced, while the melting temperature of the C_H3 domain is minimally affected. The resulting structural change leads to a lowered physical and covalent stability. Although the data reported here were obtained using an aglycosylated Fc, the results also have direct implications for glycosylated IgG antibody and Fc fusion proteins (molecules with the Fc-containing moieties). In fact, similar changes in the thermal stability of glycosylated Fc and IgG1 monoclonal antibodies have been observed (D. Liu et al., unpublished data). These results offer an excellent example of the interplay between physical and covalent stabilities and further highlight the importance of reducing or completely eliminating methionine oxidation during the manufacturing and formulation processes. The significant effect on protein stability was observed only for the highly oxidized Fc protein; therefore, it is expected that low levels of methionine oxidation present in the Fc-containing protein therapeutics will have a minimal impact, especially when the methionine oxidation is tightly controlled by the protein formulation and proper product storage conditions. Furthermore, these results provide a basis

for further exploring the mechanism of structural changes and their relationship to stability. Given the fact that the Met 33 and Met 209 residues are conserved among IgG isotypes and are involved in protein–protein interactions with protein A (*45*), protein G (*46*), rheumatoid factor (*47*), and neonatal Fc receptor (*48*), the effect of methionine oxidation on these protein–protein interactions and on Fc's *in vivo* biological functions, such as *in vivo* half-life, may also be impacted. This will be the subject of future research.

ACKNOWLEDGMENT

We thank Dr. Sampath Krishnan for useful discussions and Dr. Kenneth Walker for providing the Fc mutant protein. We also thank Liang-Yu Shih for her assistance in analyzing DSC data and Dr. Tsang-lin Hwang for his assistance in NMR measurements.

REFERENCES

1. Dalle-Donne, I., Rossi, R., Giustarini, D., Gagliano, N., Di Simplicio, P., Colombo, R., and Milzani, A. (2002) Methionine oxidation as a major cause of the functional impairment of oxidized Actin. *Free Radical Biol. Med. 32*, 927–937.
2. Sigalov, A. B., and Stern, L. J. (2001) Oxidation of methionine residues affects the structure and stability of apolipoprotein A-I in reconstituted high density lipoprotein particles. *Chem. Phys. Lipids 113*, 133–146.
3. Lu, H. S., Fausset, P. R., Narhi, L. O., Horan, T., Shinagawa, K., Shimamoto, G., and Boone, T. C. (1999) Chemical modification and site-directed mutagenesis of methionine residues in recombinant human granulocyte colony-stimulating factor: Effect on stability and biological activity. *Arch. Biochem. Biophys. 362*, 1–11.
4. Bartlett, R. K., Bieber Urbauer, R. J., Anbanandam, A., Smallwood, H. S., Urbauer, J. L., and Squier, T. C. (2003) Oxidation of Met144 and Met145 in calmodulin blocks calmodulin dependent activation of the plasma membrane Ca-ATPase. *Biochemistry 42*, 3231–3238.
5. Cleland, J. L., Powell, M. F., and Shire, S. J. (1993) The Development of Stable Protein Formulations: A Close Look at Protein Aggregation, Deamidation and Oxidation. *Crit. Rev. Ther. Drug Carrier Syst. 10*, 307–377.
6. Duenas, E. T., Keck, R., De Vos, A., Jones, A. J., and Cleland, J. L. (2001) Comparison between light induced and chemically induced oxidation of rhVEGF. *Pharm. Res. 18*, 1455–1460.
7. Kornfelt, T., Persson, E., and Palm, L. (1999) Oxidation of Methionine Residues in Coagulation Factor VIIa. *Arch. Biochem. Biophys. 363*, 43–54.
8. Lam, X. M., Yang, J. Y., and Cleland, J. L. (1997) Antioxidants for Prevention of Methionine Oxidation in Recombinant Monoclonal Antibody HER2. *J. Pharm. Sci. 86*, 1250–1255.
9. Chu, J. W., Yin, J., Brooks, B. R., Wang, D. I., Ricci, M. S., Brems, D. N., and Trout, B. L. (2004) A comprehensive picture of non-site specific oxidation of methionine residues by peroxides in protein pharmaceuticals. *J. Pharm. Sci. 93*, 3096–3102.
10. Schoneich, C. (2005) Methionine oxidation by reactive oxygen species: Reaction mechanisms and relevance to Alzheimer's disease. *Biochim. Biophys. Acta 1703*, 111–119.
11. Hermeling, S., Crommelin, D. J., Schellekens, H., and Jiskoot, W. (2004) Structure-immunogenicity relationships of therapeutic proteins. *Pharm. Res. 21*, 897–903.
12. Ghetie, V., and Ward, E. S. (2000) Multiple roles for the major histocompatibility complex class I-related receptor FcRn. *Annu. Rev. Immunol. 18*, 739–766.
13. Raghavan, M., Bonagura, V. R., Morrison, S. L., and Bjorkman, P. J. (1995) Analysis of the pH dependence of the neonatal Fc receptor/immunoglobulin G interaction using antibody and receptor variants. *Biochemistry 34*, 14649–14657.
14. Wang, B., Nichol, J. L., and Sullivan, J. T. (2004) Pharmacodynamics and pharmacokinetics of AMG 531, a novel thrombopoietin receptor ligand. *Clin. Pharmacol. Ther. 76*, 628–638.
15. Burton, D. R., and Woof, J. M. (1992) Human antibody effector function. *Adv. Immunol. 51*, 1–84.
16. Jefferis, R., Lund, J., and Pound, J. D. (1998) IgG-Fc-mediated effector functions: Molecular definition of interaction sites for effector ligands and the role of glycosylation. *Immunol. Rev. 163*, 59–76.
17. Saphire, E. O., Parren, P. W., Pantophlet, R., Zwick, M. B., Morris, G. M., Rudd, P. M., Dwek, R. A., Stanfield, R. L., Burton, D. R., and Wilson, I. A. (2001) Crystal structure of a neutralizing human IGG against HIV-1: A template for vaccine design. *Science 293*, 1155–1159.
18. Kabat, E. A., Wu, T. T., Perry, H. M., Gottesman, K. S., and Foeller, S. (1991) Sequences of proteins of immunological interest. NIH Publication 91-3242, 5th ed., National Institutes of Health, Bethesda, MD.
19. Nichol, J. L. (2006) AMG 531: An investigational thrombopoiesis-stimulating peptibody. *Pediatr. Blood Cancer 47*, 723–725.
20. Shields, R. L., Namenuk, A. K., Hong, K., Meng, Y. G., Rae, J., Briggs, J., Xie, D., Lai, J., Stadlen, A., Li, B., Fox, J. A., and Presta, L. G. (2001) High resolution mapping of the binding site on human IgG1 for Fc gamma RI, Fc gamma RII, Fc gamma RIII, and FcRn and design of IgG1 variants with improved binding to the Fc gamma R. *J. Biol. Chem. 276*, 6591–6604.
21. Shen, F. J., Kwong, M. Y., Keck, R. G., Harris, R. J., and Marshak, D. R. (1996) The application of tert-butylhydroperoxide oxidation to study sites of potential methionine oxidation in a recombinant antibody, in *Techniques in protein chemistry*, pp 275–284, Academic Press, San Diego.
22. Lam, X. M., Yang, J. Y., and Cleland, J. L. (1997) Antioxidants for prevention of methionine oxidation in recombinant monoclonal antibody HER2. *J. Pharm. Sci. 86*, 1250–1255.
23. Pipes, G. D., Kosky, A. A., Abel, J., Zhang, Y., Treuheit, M. J., and Kleemann, G. R. (2005) Optimization and applications of CDAP labeling for the assignment of cysteines. *Pharm. Res. 22*, 1059–1068.
24. Chumsae, C., Gaza-Bulseco, G., Sun, J., and Liu, H. (2007) Comparison of methionine oxidation in thermal stability and chemically stressed samples of a fully human monoclonal antibody. *J. Chromatogr., B: Anal. Technol. Biomed. Life Sci. 850*, 285–294.
25. Liu, H., Gaza-Bulseco, G., Xiang, T., and Chumsae, C. (2008) Structural effect of deglycosylation and methionine oxidation on a recombinant monoclonal antibody. *Mol. Immunol. 45*, 701–708.
26. Kamei, D. T., Speed Ricci, M., Deshpande, R., Xu, H., and Lauffenburger, D. A. (2004) Quantitative analysis of Fc ligand recycling kinetics. *Biotechnol. Bioeng. 92*, 748–760.
27. Chelius, D., Rehder, D. S., and Bondarenko, P. V. (2005) Identification and characterization of deamidation sites in the conserved regions of human immunoglobulin gamma antibodies. *Anal. Chem. 77*, 6004–6011.
28. Delaglio, F., Grzesiek, S., Vuister, G. W., Zhu, G., Pfeifer, J., and Bax, A. (1995) NMRPipe: A multidimensional spectral processing system based on UNIX pipes. *J. Biomol. NMR 6*, 277–293.
29. Johnson, B. A. (2004) Using NMRView to visualize and analyze the NMR spectra of macromolecules. *Methods Mol. Biol. 278*, 313–352.
30. Krapp, S., Mimura, Y., Jefferis, R., Huber, R., and Sondermann, P. (2003) Structural analysis of human IgG-Fc glycoforms reveals a correlation between glycosylation and structural integrity. *J. Mol. Biol. 325*, 979–989.
31. Woody, R. W. (1994) Contributions of tryptophan side chains to the far-ultraviolet circular dichroism of proteins. *Eur. Biophys. J. 23*, 253–262.
32. Sreerama, N., Manning, M. C., Powers, M. E., Zhang, J. X., Goldenberg, D. P., and Woody, R. W. (1999) Tyrosine, phenylalanine, and disulfide contributions to the circular dichroism of proteins: Circular dichroism spectra of wild-type and mutant bovine pancreatic trypsin inhibitor. *Biochemistry 38*, 10814–10822.
33. Vinci, F., Catharino, S., Frey, S., Buchner, J., Marino, G., Pucci, P., and Ruoppolo, M. (2004) Hierarchical Formation of Disulfide Bonds in the Immunoglobulin Fc Fragment Is Assisted by Protein-disulfide Isomerase. *J. Biol. Chem. 279*, 15059–15066.
34. Sreerama, N., and Woody, R. W. (2004) Computation and analysis of protein circular dichroism spectra. *Methods Enzymol. 383*, 318–351.
35. Liu, D., Cocco, M., Rosenfied, R., Lewis, J., Ren, D., Li, L., Remmele, R. L., and Brems, D. N. (2007) Assignment of backbone ^{1}H, ^{13}C and ^{15}N resonances of human IgG1 Fc (51.4 kDa). *Biomolecular NMR Assignment 1*, 233–235.

36. Tischenko, V. M., Abramov, V. M., and Zav'yalov, V. P. (1998) Investigation of the cooperative structure of Fc fragments from myeloma immunoglobulin G. *Biochemistry 37*, 5576–5581.
37. Ghirlando, R., Lund, J., Goodall, M., and Jefferis, R. (1999) Glycosylation of human IgG-Fc: Influences on structure revealed by differential scanning micro-calorimetry. *Immunol. Lett. 68*, 47–52.
38. Renrint, D., Rosenfeld, R., Li, L., Bondarenko, P., Remmele, R. L., Jr., and Liu, D. (2008) Characterization of Chemical Degradants in human IgG1 Fc produced in *E. coli* (manuscript in preparation).
39. Chu, J. W., Yin, J., Wang, D. I., and Trout, B. L. (2004) Molecular dynamics simulations and oxidation rates of methionine residues of granulocyte colony-stimulating factor at different pH values. *Biochemistry 43*, 1019–1029.
40. Yamaguchi, Y., Nishimura, M., Nagano, M., Yagi, H., Sasakawa, H., Uchida, K., Shitara, K., and Kato, K. (2006) Glycoform-dependent conformational alteration of the Fc region of human immunoglobulin G1 as revealed by NMR spectroscopy. *Biochim. Biophys. Acta 1760*, 693–700.
41. Kim, Y. H., Berry, A. H., Spencer, D. S., and Stites, W. E. (2001) Comparing the effect on protein stability of methionine oxidation versus mutagenesis: Steps toward engineering oxidative resistance in proteins. *Protein Eng. 14*, 343–347.
42. Wood, M. J., Becvar, L. A., Prieto, J. H., Melacini, G., and Komives, E. A. (2003) NMR structures reveal how oxidation inactivates thrombomodulin. *Biochemistry 42*, 11932–11942.
43. Chugha, P., Sage, H. J., and Oas, T. G. (2006) Methionine oxidation of monomeric lambda repressor: The denatured state ensemble under nondenaturing conditions. *Protein Sci. 15*, 533–542.
44. Robinson, N. E., Robinson, Z. W., Robinson, B. R., Robinson, A. L., Robinson, J. A., Robinson, M. L., and Robinson, A. B. (2004) Structure-dependent nonenzymatic deamidation of glutaminyl and asparaginyl pentapeptides. *J. Pept. Res. 63*, 426–436.
45. Deisenhofer, J. (1981) Crystallographic refinement and atomic models of a human Fc fragment and its complex with fragment B of protein A from *Staphylococcus aureus* at 2.9- and 2.8-Å resolution. *Biochemistry 20*, 2361–2370.
46. Sauer-Eriksson, A. E., Kleywegt, G. J., Uhlen, M., and Jones, T. A. (1995) Crystal structure of the C2 fragment of streptococcal protein G in complex with the Fc domain of human IgG. *Structure 3*, 265–278.
47. Corper, A. L., Sohi, M. K., Bonagura, V. R., Steinitz, M., Jefferis, R., Feinstein, A., Beale, D., Taussig, M. J., and Sutton, B. J. (1997) Structure of human IgM rheumatoid factor Fab bound to its autoantigen IgG Fc reveals a novel topology of antibody-antigen interaction. *Nat. Struct. Biol. 4*, 374–381.
48. Burmeister, W. P., Huber, A. H., and Bjorkman, P. J. (1994) Crystal structure of the complex of rat neonatal Fc receptor with Fc. *Nature 372*, 379–383.

BI702238B